Dynamic Modelling and Control Design of Advanced Photovoltaic Solar System for Distributed Generation Applications♠

Marcelo G. Molina*, Luis E. Juanicó**

** CONICET, Instituto de Energía Eléctrica, University of San Juan,*
Av. Libertador San Martín 1109 Oeste, J5400ARL, San Juan, Argentina
tel/fax: +54 264 4226444/ +54 264 4210299
e-mail: mgmolina@iee.unsj.edu.ar
*** CONICET, Centro Atómico Bariloche,*
Av. Bustillo 9500, 8400, Bariloche, Río Negro, Argentina
tel/fax: +54 294 4445100 / +54 294 4445299
e-mail: juanico@cab.cnea.gov.ar

Submitted: 09/04/2010
Accepted: 09/06/2010
Appeared: 30/06/2010

Abstract— Presently, grid-connected photovoltaic (PV) solar systems are becoming the most important application of PV systems. This trend is being increased because of the many benefits of using renewable energy sources (RES) in modern distributed (or dispersed) generation (DG) systems. This electrical grid structure imposes on the distributed generator new requirements of high quality electric power, flexibility, efficiency and reliability. This paper proposes a novel high performance power conditioning system (PCS) of a three-phase grid-connected PV system and its control scheme for applications in DG systems. The PCS utilizes a two-stage energy conversion system topology composed of a DC/DC boost converter and a diode-clamped three-level voltage source inverter (VSI) that satisfies all the stated requirements. The model of the proposed PV array uses theoretical and empirical equations together with data provided by manufacturer of PV panels, solar radiation and cell temperature among others variables, in order to accurately predict the current-voltage curve. Moreover, based on the state-space averaging method a new three-level control scheme is designed, comprising a full decoupled current control strategy in the synchronous-rotating *d-q* frame, capable of simultaneously and independently exchanging both active and reactive powers with the distribution system. Validation of models and control algorithms is carried out through digital simulations using the MATLAB/Simulink environment and implementing a 250 Wp PV experimental set-up.

Keywords: Control techniques, DC/DC boost converter, Detailed modelling, Distributed (or Dispersed) generation (DG), Photovoltaic (PV) system; Power conditioning system (PCS); Renewable energy sources (RES).

1. INTRODUCTION

The world constraint of fossil fuels reserves and the ever rising environmental pollution have impelled strongly during last decades the development of renewable energy sources (RES). The need of having available sustainable energy systems for replacing gradually conventional ones demands the improvement of structures of energy supply based mostly on clean and renewable resources. At present, photovoltaic (PV) generation is assuming increased importance as a RES application because of distinctive advantages such as simplicity of allocation, high dependability, absence of fuel cost, low maintenance and lack of noise and wear due to the absence of moving parts. Furthermore, the solar energy characterizes a clean, pollution-free and inexhaustible energy source. In addition to these factors are the declining cost and prices of solar modules, an increasing efficiency of solar cells, manufacturing-technology improvements and economies of scale (Carrasco et al., 2006).

The grid integration of RES applications based on photovoltaic systems is becoming today the most important application of PV systems, gaining interest over traditional stand-alone systems. This trend is being increased because of the many benefits of using RES in distributed (aka dispersed) generation (DG) power systems, including the favorable incentives in many countries that impact directly on the commercial acceptance of grid-connected PV systems (El-Khattam and Salama, 2004; Poullikkas, 2007). This recent paradigm of electrical grid structure imposes on the DG new

♠ This work was supported by CONICET (Argentinean National Council for Science and Technology Research) and ANPCyT (Argentinean National Agency for Scientific and Technological Promotion) under projects FONCYT PICT 2005 Cod. No. 33407 and 35782.

requirements of high quality electric power, flexibility, efficiency and reliability (Ackermann et al., 2001). Modern DG applications are increasingly incorporating new dynamic compensation issues, simultaneously and independently of the conventional active power exchange between the DG and the utility grid, including voltage control, power oscillations damping, power factor correction, and harmonics filtering among others. This tendency is expected to be augmented even more in future DG applications.

This paper describes the design, simulation and implementation of a novel high performance power conditioning system (PCS) of a three-phase grid-connected PV system and its control scheme for applications in DG systems. The proposed PCS utilizes a two-stage energy conversion system topology composed of a DC/DC boost converter and a three-level voltage source inverter (VSI) that meets all the stated requirements. The model of the proposed PV array uses theoretical and empirical equations together with data provided by manufacturer of PV panels, solar radiation and cell temperature among others variables, in order to accurately predict the characteristic curve. Moreover, based on the state-space averaging method a new three-level control scheme is designed, comprising a full decoupled current control strategy in the synchronous-rotating *d-q* frame, capable of simultaneously and independently exchanging both active and reactive powers with the distribution system. Validation of models and control algorithms is carried out through computer simulations using SimPowerSystems of MATLAB/Simulink and implementing a 250 Wp PV experimental set-up.

2. MODEL OF THE PHOTOVOLTAIC SOLAR ARRAY

The building block of the PV array is the solar cell, which is basically a p-n semiconductor junction that directly converts solar radiation into DC current using the photovoltaic effect. Fig. 1 depicts the well-known equivalent circuit of the solar cell composed of a light generated current source, a diode representing the nonlinear impedance of the p-n junction, and series and parallel intrinsic resistances (Angrist, 1971; Duffie and Beckman, 1991; Nelson, 2003).

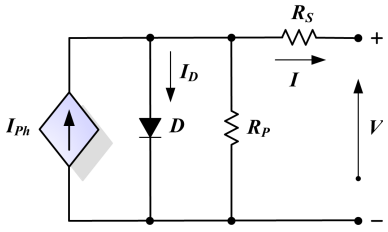

Fig. 1. Equivalent circuit of a PV cell.

PV cells are grouped together in larger units known as PV modules or arrays, which are combined in series and parallel to provide the desired output voltage and current. The equivalent circuit for the solar cells arranged in N_P-parallel and N_S-series is shown in Fig. 2. The mathematical model that predicts the power production of the PV generator becomes an algebraically simply model, being the current-voltage relationship defined in (1).

$$I_A = N_P I_{Ph} - N_P I_{RS}\left\{\exp\left[\frac{q}{AkT_C}\left(\frac{V_A}{N_S}+\frac{I_A R_S}{N_P}\right)\right]-1\right\}-\frac{N_P}{R_P}\left(\frac{V_A}{N_S}+\frac{I_A R_S}{N_P}\right) \quad (1)$$

where:

I_A: PV array output current
V_A: PV array output voltage
I_{Ph}: Solar cell photocurrent
I_{RS}: Solar cell reverse saturation current (aka dark current)
q: Electron charge, 1.60217733e–19 Cb
A: P–N junction ideality factor, between 1 and 5
k: Boltzmann's constant, 1.380658e–23 J/K
T_C: Solar cell absolute operating temperature, K
R_S: Cell intrinsic series resistance
R_P: Cell intrinsic shunt or parallel resistance

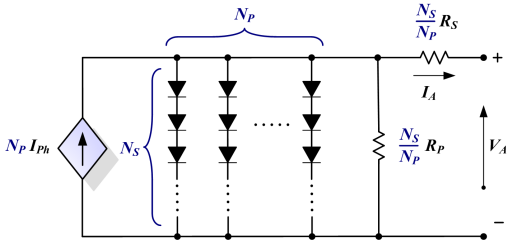

Fig. 2. Equivalent circuit of a PV array.

The photocurrent I_{Ph} for any operating conditions of the PV array is assumed to be related to the photocurrent at standard test conditions (STC) as follows:

$$I_{Ph} = f_{AM_a}\ f_{IA}\left[I_{SC} + \alpha_{Isc}\left(T_C - T_R\right)\right]\frac{S}{S_R} \quad (2)$$

where:

f_{AM_a}: Absolute air mass function describing solar spectral influence on the photocurrent I_{Ph}
f_{IA}: Incidence angle function describing influence on the photocurrent I_{Ph}
I_{SC}: Cell short-circuit current at STC
α_{Isc}: Cell temperature coefficient of the short-circuit current, A/module/diff. temp. (K)
T_R: Solar cell absolute reference temperature at STC, K
S: Total solar radiation absorbed at the plane-of-array, W/m^2
S_R: Total solar reference radiation at STC, 1000 W/m^2.

The absolute air mass function accounting for the solar spectral influence on the "effective" irradiance absorbed on the PV array surface is described through an empirically-determined polynomial function, as expressed in (3).

$$f_{AM_a} = \sum_{i=0}^{4} a_i \left(AM_a\right)^i = M_P \sum_{i=0}^{4} a_i \left(AM\right)^i \quad (3)$$

where:

a_0–a_4: Polynomial coefficients for fitting the absolute air mass function of the analyzed cell material
AM_a: Absolute air mass, corrected by pressure
AM: Atmospheric optical air mass
M_P: Pressure modifier

An algorithm for computing the solar incidence angle (*IA*) for both fixed and solar-tracking modules has been documented in Duffie and Beckman (1991). In the same way, the optical influence of the PV module surface, typically glass, was empirically described through the incidence angle function (King et al., 1998) as shown in (4) for different incident angle θ_I (in degrees).

$$f_{IA} = 1 - \sum_{i=1}^{5} b_i (\theta_I)^i \quad (4)$$

being b_1–b_5 the polynomial coefficients for fitting the incidence angle function of the analyzed PV cell material

The solar cell reverse saturation current I_{RS} varies with temperature according to the following equation:

$$I_{RS} = I_{RR} \left[\frac{T_C}{T_R} \right]^3 \exp \left[\frac{qE_G}{Ak} \left(\frac{1}{T_R} - \frac{1}{T_C} \right) \right] \quad (5)$$

where:

I_{RR}: Solar cell reverse saturation current at STC

E_G: Energy band-gap of the PV cell semiconductor at absolute temperature, T_C

As can be clearly derived from the mathematical model described by (1) through (5), the PV array exhibits highly nonlinear radiation and temperature-dependent *I–V* and *P–V* characteristic curves. This model has been simulated in the MATLAB/Simulink (The MathWorks Inc., 2009) environment using specific toolboxes and user functions. In addition, it has been experimentally validated using a 250 Wp (peak power) PV solar array implementation, composed of a string of 5 high-efficiency polycrystalline PV modules (N_S=5, N_P=1) of 50 Wp model Solartec KS50 (built with Kyocera cells). Table 1 presents the KS50 PV module technical specifications at standard test conditions (operating temperature 25ºC, solar radiation 1000 W/m^2 and absolute air mass 1.5) provided by the manufacturer and data obtained from measurements and simulations of the proposed model. All coefficients determined for this polycrystalline silicon cell PV module are provided in Table 2 in the Appendix A.

Table 1. Comparison of Solartec KS50 PV module technical specifications at standard test conditions.

Technical Specifications	Manufacturer	Measur.	Simul.
Typical Peak Power	50 Wp	49.93 Wp	49.71 Wp
Voltage at Max. Power	17.4 V	17.55 V	17.63 V
Current at Max. Power	2.87 A	2.845 A	2.82 A
Open Circuit Voltage	21.7 V	21.68 V	21.64 V
Short Circuit Current	3.13 A	3.25 A	3.33 A

Figures 3 and 4 depict the *I–V* and *P–V* characteristic curves of the 250 W PV array for different climatic conditions, such as the level of solar radiation and the cell temperature. In both figures, the characteristic curves at 25ºC and 200/600/1000 W/m^2 have been evaluated using simulations of the proposed model (blue solid line) and measurements obtained from the experimental set-up (blue dotted line). This proposed model of the PV array shows a very good agreement with measured data at all levels of solar radiation.

As can be derived from both characteristic curves of the PV system, there exist a specific point at which the generated power is maximized (also known as maximum power point or MPP) and where the output *I–V* characteristic curve is divided into two parts: the left part is defined as the current source region in which the output current approximates to a constant, and the right part is the voltage source region in which the output voltage hardly changes. Since the MPP changes with variations in solar radiation and solar cell operating temperature, the PV array have to be continuously operated within the MPP locus (shaded region) for an optimized application of the system. In this way, a continuous adjustment of the array terminal voltage is required for providing maximum power to the electric grid.

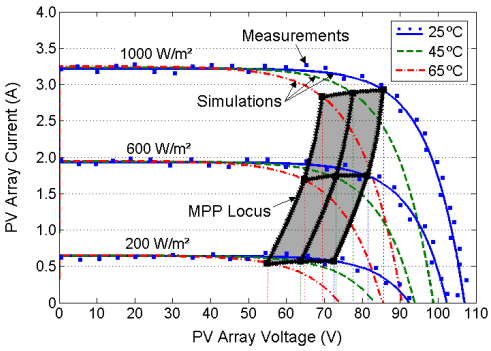

Fig. 3. Simulated and measured *I–V* curve of a string of 5 Solartec KS50 PV modules for various climatic conditions.

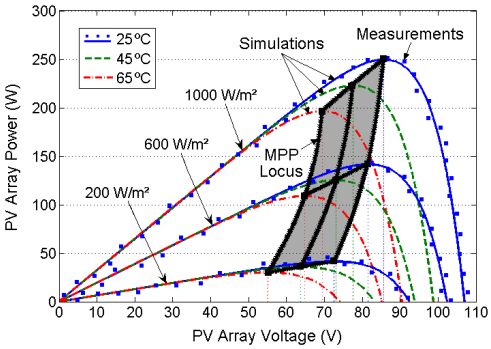

Fig. 4. Simulated and measured *P–V* curve of a string of 5 Solartec KS50 PV modules for various climatic conditions.

3. MODEL OF THE POWER CONDITIONING SYSTEM

The main purpose of a grid-connected PV solar system used as a DG is to transfer the maximum power obtained from the sun into the electric grid. This goal imposes the necessity of being constantly operating the PV system near the maximum power independently of the climatic conditions; therefore the use of an appropriate electronic interface with maximum power point tracking (MPPT) capabilities and the ability of effectively connecting to the AC power grid is required. The power conditioning system (PCS) is the electronic device that permits to achieve this objective, by successfully controlling the active power flow exchanged with the electric distribution system. Even more, with the appropriate PCS topology and its control design, the PV array is capable of simultaneously and independently performing both instantaneous active and reactive power flow control, as required by modern grid-connected DG system applications. To this aim, a hardware configuration of two cascade stages is used, which offers an additional degree of freedom in the operation of the grid-

connected PV solar system when compared with the single-stage configuration. Hence, by including the DC/DC boost converter between the PV array and the inverter linked to the electric grid, various control objectives are possible to be pursued simultaneously and independently of the PV array operation without changing the PCS topology.

The detailed model of the proposed grid-connected PV solar system is illustrated in Fig. 5, and consists of the PV solar arrangement and its PCS to the electric utility grid. PV panels are electrically combined in series to form a string (and sometimes stacked in parallel) in order to provide the desired output power required for the DG application. The full PV array is implemented using the aggregated model previously described in Fig. 2, by directly computing the total internal resistances, non-linear integrated characteristic and total generated solar cell photocurrent according to the series and parallel contribution of each parameter.

3.1 Voltage Source Inverter

The major component of the PCS is the well-known voltage source inverter (VSI) built with semiconductors devices having turn-off capabilities. This three-phase static device is shunt-connected to the distribution network by means of a coupling transformer and the corresponding line filter. Its topology allows the device to generate at the point of common coupling (PCC) to the AC network a set of three almost sinusoidal voltage waveforms at the fundamental frequency phase-shifted 120º between each other, with controllable amplitude and phase angle. Since the PV system is basically a combined stiff current-voltage source, as derived from Fig. 3, the use of a voltage source inverter is proposed because represent a more cost-effective solution.

The proposed VSI corresponds to a three-phase three-level DC/AC converter using insulated gate bipolar transistors (IGBTs). This semiconductor device is employed due to its lower switching losses and reduced size when compared to other power electronic devices. In addition, as the power rating of the inverter goes up to medium levels for typical DER applications, the output voltage control can be efficiently achieved through pulse width modulation (PWM) techniques. The connection to the utility grid is made by means of a step-up Δ–Y transformer, and second-order low pass filters are included in order to reduce the perturbation on the distribution system from high-frequency switching harmonics generated by the PWM control of the VSI.

The proposed VSI structure is designed to make use of a three-level topology called neutral point clamped (NPC). This topology generates a more smoothly sinusoidal output voltage waveform than conventional two-level structures without increasing the switching frequency and effectively doubles the power and voltage rating of the VSI for a given semiconductor device. Moreover, the three level pole attempts to address some limitations of the standard two-level by offering an additional flexibility of a level in the output voltage, which can be controlled in duration, either to vary the fundamental output voltage or to assist in the output waveform construction (Rodríguez et al., 2002). By increasing the number of levels in the converter, the output voltages waveforms have more steps generating a staircase approximation of a sinusoidal waveform, which has a reduced harmonics distortion and hence the coupling transformer could even be omitted. However, a high number of levels increases the control complexity and introduces voltage imbalance problems, voltage clamping requirements, circuit layout, and packaging constraints. In practice, the number of feasible voltage levels with adequate results is restricted to no more than five.

The proposed three-level NPC structure can be applied to reactive power generation almost without DC bus voltage imbalance problems. But when active power exchange is included, like in this proposal, the inverter could not have balanced voltages and auxiliary techniques are needed in order to provide a compensating power flow between the capacitors of the DC link (Soto and Green, 2002). For this reason, this work proposes the application of an effective control algorithm to the PWM modulation method in order to prevent VSI DC bus capacitors voltage drift/imbalance. The control algorithm employed is based on the one previously proposed in Wang and Li (2008), and consists of an interpolation method to calculate the most appropriate zero-sequence voltage to be injected into the reference voltages of the PWM modulation in order to control the neutral point (*NP*) potential voltage. This condition of *NP* voltage balancing is very significant for avoiding contributing to the AC system with additional distortion generated by the three-level inverter.

As the high-frequency harmonics produced by the inverter are mostly filtered, the VSI can be seen as an ideal sinusoidal voltage source, which is depicted in Fig. 6. This ideal inverter is shunt-connected to the network at the PCC through an equivalent inductance L_s, accounting for the leakage of the

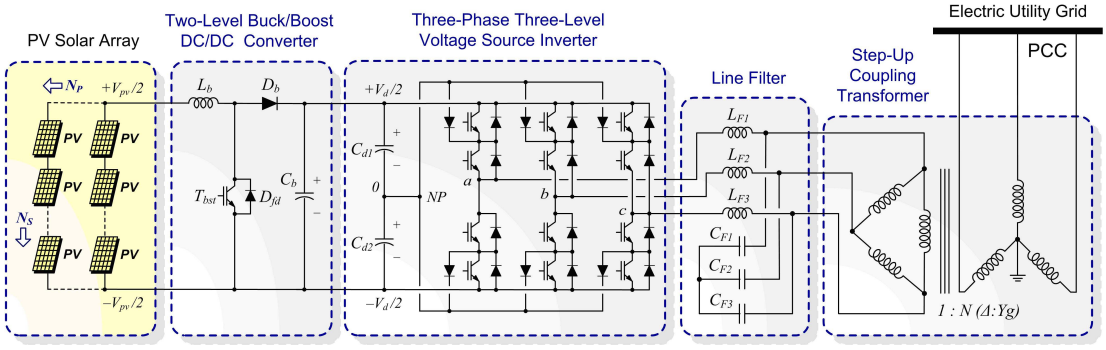

Fig. 5. Full detailed model of the proposed three-phase grid-connected photovoltaic solar system.

coupling transformer and an equivalent series resistance R_s, representing the transformers winding resistance and VSI semiconductors conduction losses. The magnetizing inductance of the step-up transformer can also be taken into consideration through a mutual equivalent inductance M. In the DC side of the VSI, losses are accounted by R_p and the equivalent capacitance of the DC bus capacitors through C_d.

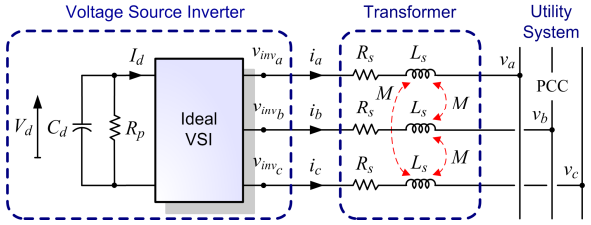

Fig. 6. Equivalent circuit diagram of the VSI connected to the AC system.

Under the assumption that the system has no zero sequence components, all currents and voltages can be uniquely transformed into the synchronous-rotating dq reference frame by applying Park's transformation. By defining the d-axis to be always coincident with the instantaneous voltage vector v_m, yields v_d equals $|v_m|$, while v_q is null. Consequently, the d-axis current component contributes to the instantaneous active power and the q-axis current component represents the instantaneous reactive power.

The dynamics equations governing the instantaneous values of the three-phase output voltages in the AC side of the VSI, the DC link voltages, and the current exchanged with the utility grid can be derived in the dq reference frame as follows (Molina et al., 2010):

$$s\begin{bmatrix} i_d \\ i_q \\ V_d \end{bmatrix} = \begin{bmatrix} \frac{-R_s}{L_s - M} & \omega & \frac{S_{av,d}}{2(L_s - M)} \\ -\omega & \frac{-R_s}{L_s - M} & \frac{S_{av,q}}{2(L_s - M)} \\ -\frac{3}{2C_d} S_{av,d} & -\frac{3}{2C_d} S_{av,q} & -\frac{2}{R_p C_d} \end{bmatrix} \begin{bmatrix} i_d \\ i_q \\ V_d \end{bmatrix} - \begin{bmatrix} \frac{|v|}{L_s - M} \\ 0 \\ 0 \end{bmatrix} \quad (6)$$

where:

$s=d/dt$: Laplace variable, defined for t > 0

ω: synchronous angular speed of the network voltage at the fundamental system frequency f (50 Hz in this work)

The average switching factors $S_{av,d}$ and $S_{av,q}$ are part of the average switching function matrix in dq coordinates, which is computed as:

$$\mathbf{S_{av,dq}} = \begin{bmatrix} S_{av,d} \\ S_{av,q} \end{bmatrix} = \frac{1}{2} m_i \; a \begin{bmatrix} \cos\alpha \\ \sin\alpha \end{bmatrix} \quad (7)$$

being,

m_i: modulation index of the VSI, $m_i \in [0, 1]$

α: phase-shift of the DSTATCOM output voltage from the reference position

$a = \sqrt{3}/\sqrt{2} \; n_2/n_1$: turns ratio of the step-up transformer

The relation between the DC side voltage V_d and the generated AC voltage v_{inv} can be described through the average switching function matrix in the dq frame $\mathbf{S_{av,dq}}$ of the inverter, as given by (8). This relation assumes that the DC capacitors voltages are balanced and equal to $V_{d/2}$.

$$\begin{bmatrix} v_{inv_d} \\ v_{inv_q} \end{bmatrix} = \mathbf{S_{av,dq}} \; V_d \quad (8)$$

3.2 DC/DC Boost Converter

The inclusion of the PV array into the DC bus of the VSI demands the use of an improved interface to adapt the wide range of variation in voltage and current levels between both devices. Controlling the PV array power generation requires varying the voltage magnitude at the PV terminals while keeping essentially constant the voltage of the VSI DC link capacitors. To this aim, a standard (two-level) unidirectional topology of IGBT DC/DC boost converter (aka step-up chopper) is employed. This intermediate converter produces a chopped output voltage through PWM techniques for controlling the average DC voltage relation between its input and output aiming at continuously matching the characteristic of the PV array to the equivalent impedance presented by the DC bus of the inverter, regardless the climatic conditions.

In steady-state continuous conduction mode, the state-space equation that describes the dynamics of the DC/DC converter is given by (9), as stated in Molina et al. (2010).

$$s\begin{bmatrix} I_g \\ V_d \end{bmatrix} = \begin{bmatrix} 0 & -\frac{(1-D)}{L_b} \\ -\frac{(1-D)}{C_d} & 0 \end{bmatrix} \begin{bmatrix} I_g \\ V_d \end{bmatrix} + \begin{bmatrix} \frac{1}{L} & 0 \\ 0 & -\frac{1}{C} \end{bmatrix} \begin{bmatrix} V_g \\ I_d \end{bmatrix} \quad (9)$$

where:

I_g: Chopper input current, or PV output current

V_g: Chopper input voltage, or PV output voltage

V_d: Chopper output voltage, or VSI DC bus voltage

I_d: Chopper output current, or VSI DC bus input current

D: duty cycle of the boost DC/DC converter, $D \in [0, 1]$, defined as the ratio of time during which the IGBT is turned-on to the period of one complete switching cycle, T_s

In the same way, assuming a constant DC output voltage of the boost converter, the steady state input-to-output voltage and current conversion relationships of the boost converter, are given by (10) and (11), respectively.

$$V_d = \frac{V_{pv}}{(1-D)} \quad (10)$$

$$I_d = (1-D)\, I_g \quad (11)$$

4. PROPOSED CONTROL STRATEGY

The proposed hierarchical control of the three-phase grid-connected PV system consists of an external, middle and internal level, as depicted in Fig. 7.

4.1 External Level Control

The external level control, which is outlined in Fig. 7 (left side) in a simplified form, is responsible for determining the active and reactive power exchange between the PV system and the utility electric system. This control strategy is designed for performing two major control objectives, namely the voltage control mode (VCM) with only reactive power compensation capabilities and the active power control mode (APCM) for dynamic active power exchange between the PV array and the electric power system. To this aim, the instantaneous voltage at the PCC is computed by employing a synchronous-rotating reference frame. In consequence, by applying Park's transformation, the instantaneous values of the three-phase AC bus voltages are transformed into *d-q* components, v_d and v_q respectively, and then filtered to extract the fundamental components, v_{d1} and v_{q1}. Since the *d*-axis is always synchronized with the instantaneous voltage vector v_m (v_{d1} equals $|v_m|$ and v_{q1} is null), the *d*-axis current component of the VSI contributes to the instantaneous active power p while the *q*-axis current component represents the instantaneous reactive power q. Thus, to achieve a full decoupled active and reactive power control, it is required to provide a decoupled control strategy for i_{d1} and i_{q1}. In this way, only v_d is used for computing the resultant current reference signals required for the desired PV output active and reactive power flows. Independent limiters are use for restrict both the power and current signals before setting the references i_{dr1} and i_{qr1}. Additionally, the instantaneous actual output currents of the PV system, i_{d1} and i_{q1}, are computed for use in the middle level control. In all cases, the signals are filtered by using second-order low-pass filters to obtain the fundamental components employed by the control system. A phase locked loop (PLL) is used for synchronizing, through the phase θ_s, the transformations from *abc* to *dq* components in the voltage and current measurement system.

The standard control loop of the external level is the VCM and consists in controlling (supporting and regulating) the voltage at the PCC through the modulation of the reactive component of the inverter output current, i_{q1}. It is significant to note that, since only reactive power is exchanged with the grid in this control mode, there is no need for the PV array or any other external energy source. In fact, this reactive power is locally generated just by the inverter and can be controlled simultaneously and independently of the active power generated by the PV array. The design of the control loop in the rotating frame employs a standard proportional-integral (PI) compensator including an anti-windup system. This control mode eliminates the steady-state voltage offset via the PI compensator. A voltage regulation droop R_d is included in order to allow the terminal voltage of the PV inverter (PCC) to vary in proportion with the compensating reactive current. Thus, the PI controller with droop characteristics becomes a simple phase-lag compensator (LC_1).

The main objective of the grid-connected solar photovoltaic generating system is to exchange with the electric utility grid the maximum available power for the given climatic conditions, independently of the reactive power generated by the inverter. In this way, the APCM allows dynamically controlling the active power flow by constantly matching the active power exchanged by the inverter with the maximum instant power generated by the PV array. As previously described, it implies a continuous knowledge of not only the PV panel internal resistances but also the voltage generated, which is very difficult to carry out and would increase complexity and costs to the DG application, since additional sensing of the cell temperature and solar radiation jointly with precise data of its characteristic curve would be required. Even more, PV parameters vary with time, this making more difficult the real-time prediction. As a result, this work proposes to implement an indirect approach which is very efficient and robust in tracking the MPP of solar photovoltaic systems (Molina et al., 2007). The proposed MPPT strategy uses a simple structure and few measured variables for implementing an iterative method that permits matching the load to the output impedance of the PV array. This objective is fulfilled with a MPP tracker that employs a "Perturbation and Observation" (P&O) method for adjusting the DC/DC converter duty cycle. This MPPT algorithm operates by constantly perturbing, i.e. increasing or

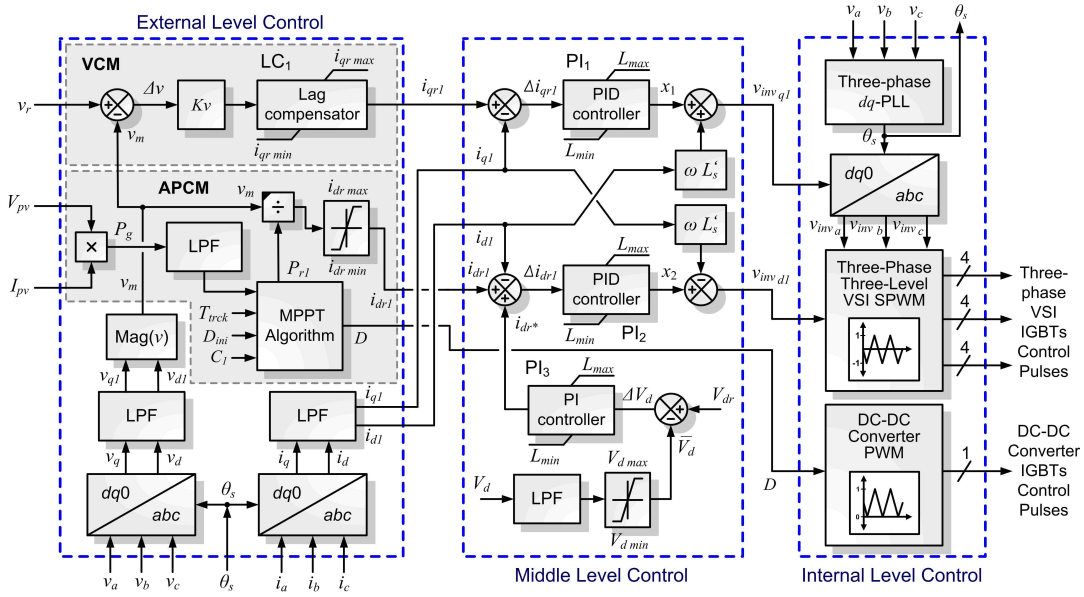

Fig. 7. Proposed multi-level control scheme for the three-phase grid-connected PV system.

decreasing, the output voltage of the PV array via the DC/DC boost converter duty cycle D and comparing the actual output power with the previous perturbation sample. If the power is increasing, the perturbation will continue in the same direction in the following cycle, otherwise the perturbation direction will be inverted. This means that the PV output voltage is perturbed every MPPT iteration cycle k at sample intervals T_{trck}, while maintaining always constant the VSI DC bus voltage by means of the middle level control. Therefore, when the optimal power for the specific operating conditions is reached, the P&O algorithm will have tracked the MPP and then will settle at this point but oscillating slightly around it. The output power measured in every iteration step is employed as a reference power signal P_{r1} and then converted to a direct current reference i_{dr1} for the middle level control.

4.2 Middle Level Control

The middle level control makes the expected output, particularly the actual active and reactive power exchange between the PV VSI and the AC system, to dynamically track the reference values set by the external level. This level control, which is depicted in Fig. 7 (middle side), is based on a linearization of the state-space mathematical model of the PV system in the *d-q* reference frame, described in (6).

In order to achieve a decoupled active and reactive power control, it is required to provide a full decoupled current control strategy for i_d and i_q. Inspection of (6) shows a cross-coupling of both components of the PV VSI output current through ω. Therefore, in order to decouple the control of i_d and i_q, appropriate control signals have to be generated. To this aim, it is proposed the use of two control signals x_1 and x_2, which are derived from assumption of zero derivatives of currents in the upper part (AC side) of (6). In this way, using two conventional PI controllers with proper feedback of the VSI output current components (PI_1 and PI_2) allows fully eliminating the cross-coupling effect in steady state. Assessment of (6) also shows an additional coupling of derivatives of i_d and i_q with respect to the DC voltage V_d. This issue requires maintaining the DC bus voltage as constant as possible in order to decrease the influence of the dynamics of V_d. The solution to this problem is obtained by using a DC bus voltage controller via a PI controller (PI_3) for eliminating the steady-state voltage variations at the DC bus. This DC bus voltage control is achieved by forcing a small active power exchange with the electric grid for compensating the VSI switching losses and the transformer ones, through the contribution of a corrective signal i_{dr*}.

4.3 Internal Level Control

The internal level provides dynamic control of input signals for the DC/DC and DC/AC converters. This control level (right side of Fig. 7) is responsible for generating the switching signals for the twelve valves of the three-level VSI, according to the control mode (PWM) and types of valves (IGBTs) used. This level is mainly composed of a line synchronization module, a three-phase three-level carrier-based (sinusoidal) PWM firing pulses generator for the VSI IGBTs, including *NP* voltage control capabilities, and a two-level PWM generator for the single IGBT of the boost DC/DC converter. The line synchronization module consists mainly of a phase locked loop (PLL). This circuit is a feedback control system used to automatically synchronize the device switching pulses; through the phase θ_s of the inverse coordinate transformation from *dq* to *abc* components, with the positive sequence components of the AC voltage vector at the PCC.

5. DIGITAL SIMULATIONS AND EXPERIMENTAL RESULTS

5.1 Simulation Results

The full detailed model of the proposed three-phase grid-connected PV energy conversion system is implemented in the MATLAB/Simulink software environment (The MathWorks Inc., 2009) and uses the SimPowerSystems (SPS), as depicted in Fig. 8. Since the detailed model of the proposed RES-based DG application contains many states and non-linear blocks such as power electronics switches, the discretization of the electrical system with fixed-step is required so as to reduce the computation effort and thus to improve the simulation performance with comparable accuracy to continuous variable-step integration algorithms. Since the precision of the simulation is controlled by the time step chosen for the discretization, two sample times are

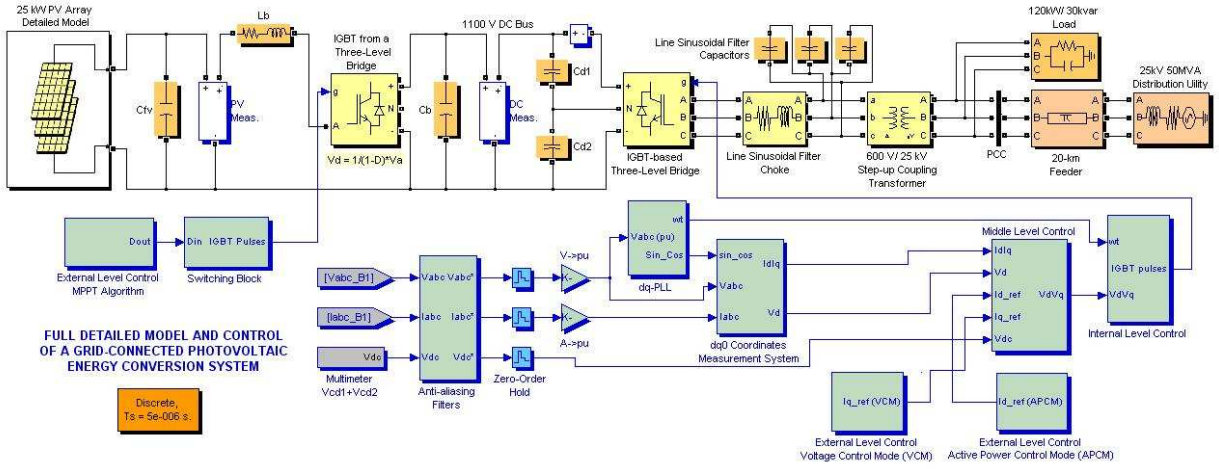

Fig. 8. Detailed model and control scheme of the grid-connected PV solar system in the MATLAB/Simulink environment.

employed as a compromise for the largest acceptable time with the sufficient precision. A sample time of 5 µs for the simulation of the power system and the PCS, and 100 µs for the simulation of the multi-level control blocks.

The three-phase grid-connected PV energy conversion system is implemented basically with the three-level bridge block. The three-phase three-level VSI makes uses of three arms of IGBTs. In the same way, the DC/DC converter is implemented through the same three-level bridge but using only one arm of IGBTs. From the four power switching devices of each arm, just one device is activated for accomplishing the chopping function while the other three are kept off all the time. With this implementation approach, the turn-on and turn-off times of the IGBTs are not modeled, resulting in a faster simulation when compared to a single IGBT mask using an increased state-space model.

In order to investigate the effectiveness of the proposed models and control algorithms of the three-phase grid-connected PV system used as a DG system, dynamic simulations with independent control of active and reactive powers exchanged between the PV system and the electric grid are carried. To this aim, two sets of simulations are performed using both control strategies of the PV-based DG system, viz. APCM and VCM. Under this scenario, a 25 kV/50 MVA distribution utility feeds a 120 kW/30 kvar load via a 20 km line. The PV array consists of 10 strings of 50 modules ($N_S=50$, $N_P=10$), making up a peak installed power of 25 kW, linked to a 1100 V DC bus of the inverter through the DC/DC boost converter. The connection of the VSI to the utility grid is made through a 600 V/25 kV step up transformer. The three-phase grid-connected PV system is simulated, under changing solar radiation conditions while maintaining the module operating temperature at 25 ºC.

Simulations depicted in Fig. 9 show the case with only active power exchange with the utility grid, i.e. only the APCM is activated all the time. The solar radiation is forced to vary quickly in steps every 0.2 s as described in Fig. 9(a), producing changes in the maximum power drawn from the PV array, as derived from Fig. 9(b). The true maximum power point for each solar radiation condition is given by the actual produced power, which is rapidly and accurately tracked by the P&O MPPT method. The trade-off between fast MPP tracking and power error in selecting the appropriate size of the perturbation step can be notably optimized in efficiency. In this work, this step was optimized in accordance with the designed DC/DC chopper dynamics, yielding a sampling interval T_{trck} of 1 ms and a ΔD of 0.005 with excellent results. The instantaneous duty cycle during the MPP tracking is shown in Fig. 9(c). In the same way, Fig. 9(d) through Fig. 9(e) shows the variations of the instantaneous voltage at the point of coupling to the distribution feeder (PCC) and the VSI DC link capacitor voltages V_{c1} and V_{c2}. As can be observed, the DC link capacitor voltages are balanced and controlled in an efficient way due to the *NP* voltage control algorithm employed. As can be noted from Fig. 9(f), all the active power generated by the PV array is injected into the electric grid, except losses, while no reactive power is locally generated by the power

(a) Solar radiation

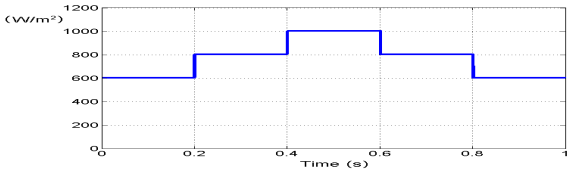

(b) Actual vs. P&O estimated PV array power

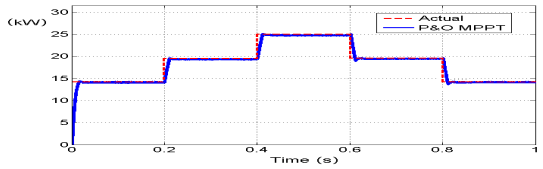

(c) Boost DC/DC converter duty cycle

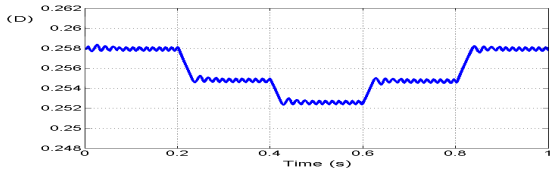

(d) DC bus capacitors voltage, V_{c1} and V_{c2}

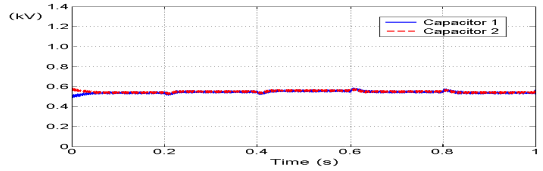

(e) VSI output voltage, v_d

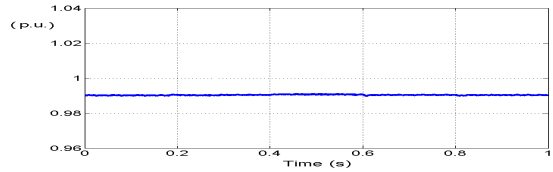

(f) VSI output active and reactive power, *P* and *Q*

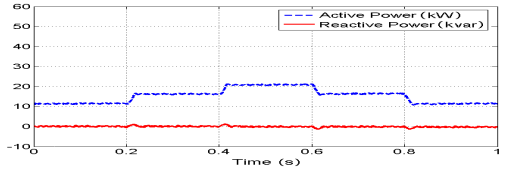

Fig. 9. Simulation results for active power exchange with the utility grid (APCM).

inverter. The voltage at the PCC is maintained almost invariant at 0.99 p.u. (base voltage of 25 kV). It is also verified a very low transient coupling between the active and reactive (null in this operating state) powers exchanged by the grid-connected PV system due to the proposed full decoupled current control strategy in *d-q* coordinates.

Simulations of Fig. 10 show the case with both, active and reactive powers exchange with the utility grid, i.e. the APCM is activated all the time while the VCM is activated at t=0.3 s. The PV array is now subjected to the same previous profile of solar radiation variations, as described in Fig. 10(a). As can be seen from Fig. 10(b), the maximum power for each solar radiation condition is rapidly and accurately drawn by the P&O MPPT method in the same way as in the previous case study, with almost similar instantaneous duty cycle trajectory for MPP tracking, as depicted in Fig. 10(c). Since the DC bus

(a) Solar radiation

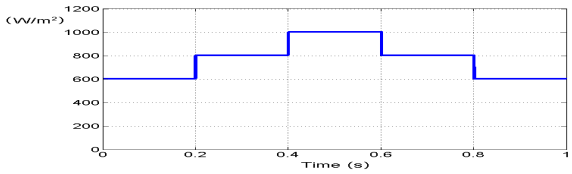

(b) Actual vs. P&O estimated PV array power

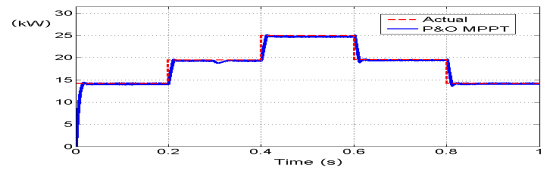

(c) Boost DC/DC converter duty cycle

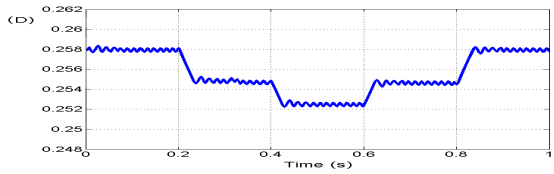

(d) DC bus capacitors voltage, V_{c1} and V_{c2}

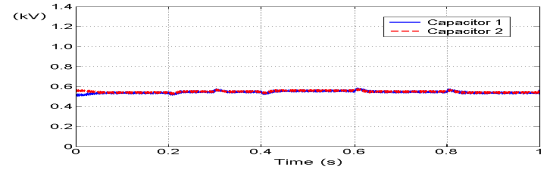

(e) VSI output voltage, v_d

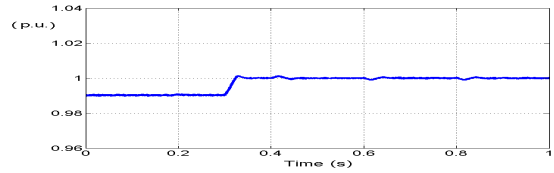

(f) VSI output active and reactive power, P and Q

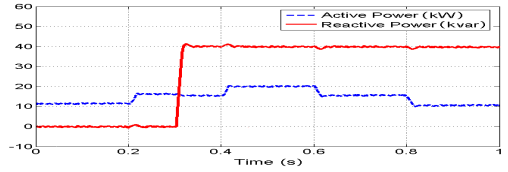

Fig. 10. Simulation results for active and reactive power exchange with the utility grid (APCM and VCM).

voltage is regulated at a constant level of 1100 V and independent of the power exchanged with the electric system, the DC side of the PV PCS is virtually isolated from the AC side. In this way, all DC variables remain unchanged with respect to the prior case study, such as the balancing and control of the DC bus capacitor voltages V_{c1} and V_{c2} (Fig. 10(d)). The modulation index of the VSI is controlled from t=0.3s in order to increase the magnitude of the instantaneous voltage at the PCC from 0.99 p.u. up to 1 p.u by exchanging almost 40 kvar of reactive power (Fig. 10(e) through Fig. 10(f)). As can be also noted, all the active power generated by the PV array is injected into the electric grid, except losses. These losses are increased with the injection of reactive power, causing a lower exchange of active power than the previous case studied. Here it is also verified a very low transient coupling between the active and reactive powers injected into the AC grid due to the full decoupled current control strategy in the *d-q* reference frame.

5.2 Experimental Evaluation

A 250 Wp laboratory-scale prototype was implemented in order to perform an experimental analysis of the actual performance of the proposed PV energy conversion system. The PV array, a string of 5 (series-connected) 50 Wp Solartec KS50 polycrystalline PV modules, is connected to a 380 V three-phase electric system through a 1 KVA 5 kHz three-level PWM inverter with a 110 V DC bus. To this aim, a DC/DC boost converter is used as interface between the PV array and the VSI for achieving the input-output voltage requirements while tracking the maximum power point. The proposed MPPT algorithm was implemented by using the high-performance digital signal processor (DSP) of Texas Instruments, TMS320F2812 which allows obtaining very small duty cycle perturbation steps, as the employed in previous simulations.

Temperature and solar radiation data for a 5-day full period were measured with intervals of 1 minute using a Davis Vantage Pro Plus weather station, as illustrated in Fig. 11. From the data collected, the study was focused on the 10-hour period identified with a dashed red circle, because it corresponds to a cloudy day with high fluctuations of solar radiation.

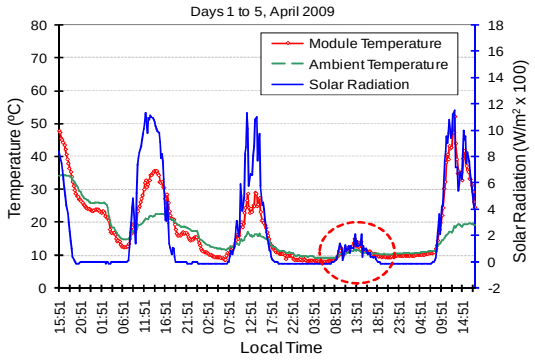

Fig. 11. Temperature and radiation data for a 5-day period.

Fig. 12 presents a comparison of actual, measured and simulated output power trajectory within the period of analysis, for the proposed 250 W PV system with and without the implementation of the MPPT algorithm. The time data series shown in light blue solid line represents the actual maximum power available from the PV array for the specific climatic conditions, i.e. the maximum power point to be tracked at all times. Simulations obtained with the proposed models and control schemes including the MPPT algorithm are shown in red solid lines and were exported straightforwardly from the Simulink environment. In the same way, the two time data series shown in black and green solid lines, respectively, represents the measurements obtained from the experimental setup with the control system with the MPPT activated (black) and with no MPPT (green). As can be observed, the MPPT algorithm follows accurately the maximum power that is proportional to the solar radiation and temperature variations. In this sense, it can be noted a very precise MPP tracking when soft variations in the solar

radiation take place, while differing slightly when these variations are very fast and of a certain magnitude. It can be also derived from the results obtained that there is a good correlation between the experimental and the simulation data. In addition, the deactivation of the MPPT control results in a constant voltage operation of the PV array output at about 60 V for the given prototype conditions. In this last case, a significant reduction of the installation efficiency is obtained, which is worsen with the increase of the solar radiation. This preceding feature validates the use of an efficient MPPT scheme for maximum exploitation of the PV system.

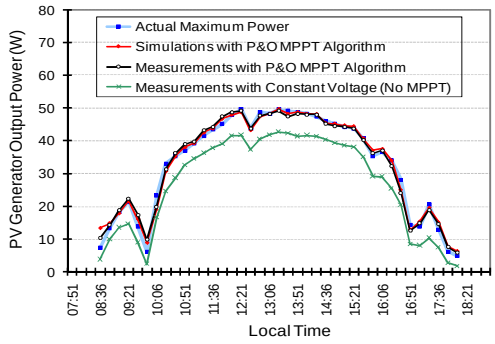

Fig. 12. Comparison of actual, measured and simulated output power trajectory for the proposed 250 W PV system with and without the MPPT algorithm implementation.

6. CONCLUSION

A detailed mathematical model and a new multi-level control scheme of a three-phase grid-connected PV system for DG applications have been proposed. The proposed model of the PV array uses theoretical and empirical equations together with data provided by the manufacturer and meteorological in order to accurately predict the module characteristic curve. The control algorithms incorporate a maximum power point tracker (MPPT) for dynamic active power generation jointly with reactive power compensation of distribution utility system. Dynamic system simulation studies demonstrate the effectiveness of the proposed multi-level control approaches and the detailed models presented. Moreover, a small-scale PV experimental set-up was employed to demonstrate the accuracy of proposed systems.

REFERENCES

Ackermann, T.; Anderson, G. and Söder L. (2001). Distributed generation: a definition, *Electric Power Systems Research*, vol. 57, pp. 195–204.

Angrist, S.W. (1971). *Direct Energy Conversion*, 2nd Ed., Allyn and Bacon, Boston.

Carrasco, J.M.; Franquelo, L.G.; Bialasiewicz, J.T.; Galván, E.; Portillo-Guisado, R. C.; Martín-Prats, M. A.; León, J. I.; Moreno-Alfonso, N. (2006). Power electronic systems for the grid integration of renewable energy sources: a survey. *IEEE Trans. Industrial Electronics*, vol. 53, no. 4, pp.1002–1016.

Duffie, J.A. and Beckman, W.A. (1991). *Solar Engineering of Thermal Processes*, 2nd Ed., John Wiley & Sons, New York.

El-Khattam, W.; Salama, M.M.A. (2004). Distributed generation technologies: definitions and benefits. *Electric Power Systems Research*, vol. 71, pp. 119–128.

King, D.L.; Kratochvil, J.A.; Boyson, W.E.; Bower, W.I. (1998). Field experience with a new performance characterization procedure for photovoltaic arrays. *Proc. 2nd World Conf on Photovoltaic Solar Energy Conversion*, vol. 1, pp. 6–10.

Molina, M.G.; Juanicó, L.E.; Rinalde G.F.; Taglialavore, E.; Gortari, S. (2010). Design of Improved Controller for Thermoelectric Generator used in Distributed Generation. *Int. Journal of Hydrogen Energy*, vol.35, no. 11, pp. 5968–5973.

Molina, M.G.; Pontoriero, D.H. and Mercado, P.E.. (2007). An efficient maximum-power-point-tracking controller for grid-connected photo-voltaic energy conversion system. *Brazilian Journal of Power Electronics*, vol. 12, no. 2, pp.147–154.

Nelson, J. (2003). *The Physics of Solar Cells*. Imperial College Press, London.

Poullikkas, A. (2007). Implementation of distributed generation technologies in isolated power. *Renewable and Sustainable Energy Reviews*, vol. 11, pp. 30–56.

Rodríguez, J.; Lai, J.S. and Peng, F.Z (2002). Multilevel inverters: a survey of topologies, controls, and applications. *IEEE Trans. Industrial Electronics*, vol. 49, no. 4, pp.724–738.

Soto, D. and Green, T.C. (2002). A comparison of high-power converter topologies for the implementation of FACTS controllers. *IEEE Trans. Industrial Electronics*, vol. 49, no. 5, pp.1072–1080.

The MathWorks Inc. (2009). *SimPowerSystems for use with Simulink 7: User's Guide*, Natick, MA.

Wang, C. and Li, Y. (2008). A new balancing algorithm of neutral-point potential in the three-level NPC converters. *Proc. IEEE Industry Appl. Society Annual Meeting*, vol. 1, pp. 1–5.

Appendix A

Table 2. Parameters determined for the Solartec KS50 PV solar module at standard test conditions.

f_{AM_a} coeff.	Values	f_{IA} coeff.	Values
a_0	0.9326	b_1	2.439e–3
a_1	6.25e–2	b_2	–3.101e–4
a_2	–1.06e–2	b_3	1.244e–5
a_3	1.415e–3	b_4	–2.110e–7
a_4	–6.155e–5	b_5	1.397e–9

AUTHORS PROFILE

Marcelo G. Molina was born in San Juan, Argentina. He graduated as Electronic Engineer from the National Universty of San Juan (UNSJ), Argentina in 1997, and received the Ph.D. degree from the UNSJ in 2004. During 2004, he was a Doctoral Fellow from CAPES at the Federal University of Rio de Janeiro, Brazil. From 2005 to 2007 he worked as a Post-Doc Research Fellow at the UNSJ. In 2009 he was a visiting professor at the University of Siegen, Germany, sponsored by DAAD. Since 2004, Dr. Molina is an Associate Professor at the UNSJ and Researcher of the Argentinean National Council for Science and Technology Research (CONICET). His research interests include new energy technologies, simulation methods, power systems dynamics and control, power electronics modeling and design, renewable energy resources and the application of energy storage in power systems.

Luis E. Juanicó is an Argentinean researcher highly interesed in new energy technologies, with many inventions in the subjects of solar thermal, nuclear fuel and uranium enrichment for nuclear reactors, thermoelectric generators, motor engines cogeneration and petroleum crude oil purification. In these areas he have produced more than 50 technical papers and he has claimed 12 invention patents. Dr. Juanicó was graduated in Nuclear Engineer in the Balseiro Institute (National University of Cuyo) at 1991, obtaining similarly his Ph.D. degree in 1998. Working in the Argentinean National Atomic Comission (CONEA) until 2001, he worked at Perez Companc, an latinamerican Oil&Gas company until 2004, and after that, he is working today as independent researcher in technology of the CONICET at the Bariloche Atomic Center, and assistant teacher of the Balseiro Institute.